ECCOMAS Congress 2016
VII European Congress on Computational Methods in Applied Sciences and Engineering
M. Papadrakakis, V. Papadopoulos, G. Stefanou, V. Plevris (eds.)
Crete Island, Greece, 5–10 June 2016

DYNAMICS OF WIND TURBINE BLADES USING A GEOMETRICALLY-EXACT BEAM FORMULATION

Celso Jaco Faccio Júnior[1], **Alfredo Gay Neto**[1]

[1]Polytechnic School at University of São Paulo
Av. Prof. Almeida Prado tv. 2, n. 83
celsojf@gmail.com, alfredo.gay@usp.br

Keywords: Wind Turbine, Blade, Beam, Finite Element Method.

Abstract. *On wind energy context, the blades of horizontal axes wind turbines have, in their majority, a closed multicellular thin-walled cross section, which varies along the blade length due to aerodynamic requirements. If one wants to analyze the structural behavior of such blades, a dynamic model is necessary. Such models are desirable, since it is important the development of lighter and more flexible wind turbine designs. The desirable results of the models include evaluating the possible large deflections along time, the internal loads along the blade length and natural frequencies experimented by the structure. Moreover, one can address the magnitude and frequency of the reactions lying at the top of the turbine tower structure, due to the action of the blades. In order to model the blades with a small number of degrees of freedom, geometrically-exact beam elements are employed. The equivalent properties to be input in the model, however, are not straightforward to be obtained. This is one of the goals of the present work. A pre-processor was developed to evaluate the cross sections properties of a wind turbine blade. It calculates all the necessary input data to represent the blade as an equivalent beam and, generates an input file with data of the model to be solved in the geometrically-exact GIRAFFE dynamic simulator. Since dealing with multicellular thin-walled cross section, it is important to evaluate the centroid, the barycenter, the shear center, the inertia properties, and the equivalent specific mass. All these properties may vary along the blade length. It is possible to manipulate the blade profile, changing the number of cells, thickness, materials involved, shape of the external shell and webs positioning. The developed pre-processor, together with the dynamic simulator, can be used to predict large displacements in a dynamic simulation of wind turbines.*

1 INTRODUCTION

The idea of using the kinetic energy provided from wind is not new. There are registers of windmills dated even from medieval times. However, the current increase for energy demand, has made of the wind energy one of the most important renewable energy resources. One of the issues raised during the last years is the structural design that best fits on the role of extracting the kinetic energy from wind. Although many innovative designs are being proposed, the most common still used is the horizontal axis wind turbine (HAWT).

HAWT are structures which usually are made by some slender bodies, composed mainly by a foundation, a tower, a nacelle a rotorhub and blades. It comes that HAWT have been presenting good results on energy production. Although many issues, such as the local wind flow may affect an HAWT, it has been seen that the energy production is directly associated with the diameter of the rotor and the design of the blades. As expected, a large rotor diameter produces more energy. For example, a HAWT 41 m rotor diameter may produce 600 kW, while a 66 m rotor may produce up to 1500 kW (Hau, 2013). Unlikely the rotor diameter, there is no straightforward relation between the blades airfoil design and the energy production. In fact, the relation between the shape of the blade and the energy production is much more complex and plays a major role, since it is the structure responsible for extracting the wind energy. The blade shape is influenced by aspects such as:

- Rotor diameter;
- Aerodynamic loads;
- Gravitational loads;
- Fluid structure interaction;
- Others.

An accurate modeling of those aspects should result in a structure able not just to resist to internal and external forces, but also that has the best use of the materials and gives the minimum maintenance. It follows that modern blade of HAWT's are becoming more slender, more flexible and composite made. All of those questions lead to a huge complexity when modeling and simulating HAWT. These models should be able to handle dynamics, nonlinearities and instability.

Deal with all the variables that compose the problem on a high-hierarchy context (e.g.: finite elements solids) may result on non-practical solution time and on hard to evaluate inputs and outputs. On the other hand, beam-like modeling presents, generally, fast solution time and easier to handle inputs and outputs. Although beam-like models present some simplifications, a huge amount of works proves that they are very representative and still useful.

Despite of the inherent simplifications, there are different beams theories that may apply, accordingly to the problem to be solved. Depending on the slenderness and on the cross section characteristics, one may choose to represent the structure using the Bernoulli-Euler beam, the Timoshenko beam, the Vlasov's beam (when warping plays a role), among other theories - refer to (Gere and Timoshenko, 1997), (Timoshenko and Goodier, 1951) and (Vlasov, 1961) for the classical theories here referenced.

1.1 The geometrically-exact beam model

When presenting the distinct beam theories, always one has a kinematic assumption regarding the behavior of the beam cross-sections. The Bernoulli-Euler beam theory is known as the classic beam theory. Their main assumption is that the beam cross-section moves as a rigid body and that it keeps orthogonal to the beam axis. On the Timoshenko beam theory the beam cross-section has rotation degrees of freedom around the beam axis, leading to distortion due to shear. The Timoshenko-Vlasov theory has the non-uniform Vlasov torsion in addition to the Timoshenko beam theory hypothesis. Therefore, it is necessary to introduce the concept of bimoment and bishear as a consequence of the non-uniform torsion of the beam.

The geometrically-exact beam theory may consider Bernoulli-Euler, Timoshenko or more elaborated kinematic assumptions of the cross-section. The main feature of such model is that the cross-section movement may present finite rotations and large translations in space. We here mention some works, basis of current developments: the first developments on this theory were presented on Simo (1985), Simo and Vu Quoc (1991) and Pimenta and Yojo (1993). Although the rotation tensors were expressed by Yojo (1993) using the Euler parameters, the development using Rodrigues parameters were after presented on Pimenta and Campello (2001).

The geometrically-exact beam theory plays a very important role on high-nonlinear engineering structures, such as offshore risers and slender wind turbines. A geometrically-exact model for static offshore risers for oil exploitation was presented by Gay Neto et al. (2014a), which was used to study the riser stability under torsion by Gay Neto and Martins (2013), Gay Neto et al. (2014b) and Wriggers et al. (2015). On these models, the contact between the riser and the seabed is considered, and in some cases a rolling beam to flat surface contact model is used, as presented by Gay Neto et al. (2014a).

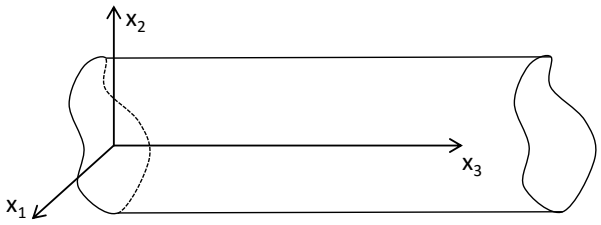

Figure 1: Beam axis notation.

Although all the complexity involved on the development of the geometrically-exact beam formulation, a linear constitutive equation regarding the cross section of a warping-free beam element is given by:

$$\boldsymbol{\sigma} = \boldsymbol{D}\boldsymbol{\varepsilon}, \tag{1}$$

where $\boldsymbol{\sigma}$ is a vector that collects the generalized stresses (internal loads) of the beam and is defined as:

$$\boldsymbol{\sigma} = \begin{bmatrix} N_1 \\ N_2 \\ N_3 \\ M_1 \\ M_2 \\ M_3 \end{bmatrix}, \tag{2}$$

where N_1, N_2 and N_3 are the components of the internal force and M_1, M_2 and M_3 are the components of the internal moment. The variable $\boldsymbol{\varepsilon}$ is a vector that collects the generalized strains of the beam and is defined as

$$\boldsymbol{\varepsilon} = \begin{bmatrix} \eta_1 \\ \eta_2 \\ \eta_3 \\ \kappa_1 \\ \kappa_2 \\ \kappa_3 \end{bmatrix}, \tag{3}$$

and $\boldsymbol{D}$ is the constitutive matrix of the beam as follows

$$\boldsymbol{D} = \begin{bmatrix} GA & 0 & 0 & 0 & 0 & G(S_1^s - S_1) \\ 0 & GA & 0 & 0 & 0 & G(-S_2^s + S_2) \\ 0 & 0 & EA & ES_1 & -ES_2 & 0 \\ 0 & 0 & ES_1 & EI_{11} & -EI_{12} & 0 \\ 0 & 0 & -ES_2 & -EI_{12} & EI_{22} & 0 \\ G(S_1^s - S_1) & G(-S_2^s + S_2) & 0 & 0 & 0 & GI_t \end{bmatrix}, \tag{4}$$

where E is the material Young Modulus, G is the material Shear Modulus, A is the beam cross-section area, S is the first order moment of inertia, I is the second order moment of inertia, I_t is the torsion stiffness and S_1^s and S_2^s are given by:

$$S_1^s = A(g_2 - s_2) \tag{5}$$

$$S_2^s = A(g_1 - s_1), \tag{6}$$

where the (g_1, g_2) are cross-section centroid coordinates and (s_1, s_2) are the shear center coordinates. The subscript numbers indicate from which axis the property is calculated and the 12 subscript is used to refer to the product of inertia. Figure 2 presents a generic beam section located at an arbitrary point $\boldsymbol{O}$, the centroid $\boldsymbol{g}$ in green and the shear center $\boldsymbol{s}$ in red.

1.2 Wind Turbine Blade Cross-Section Profiles

As commented in Section 1, HAWT blades design may be very complex due to all the requirements that it should satisfy such as the dynamic loads, the materials involved, the manufacturing process and others. Due to all of these needs it is very common to have blades with varying cross sections along their length. This solution permits each blade section to be designed according to their specific requirements. It is also very common the usage of two webs,

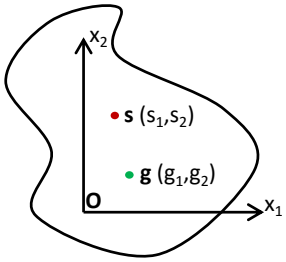

Figure 2: Beam cross-section.

in order to improve the mechanical properties of the cross section. A typical HAWT blade profile is presented in Figure 3, where one may observe an outer shell in black color and two webs in red color.

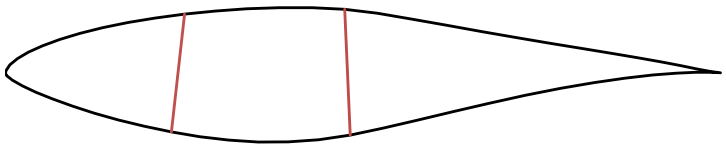

Figure 3: Typical HAWT blade profile.

The first profiles used on HAWT blades were designed by the Nation Advisory Committee for Aeronautics (NACA). The results, however, were not as expected. It was proved then that an aeronautical profile is not necessarily the best profile for an HAWT (Burton et al., 2011).

The early developments of profiles for specific use on HAWT began with a partner work with the National Renewable Energy Laboratory (NREL) and Tangler and Somers (1995). This work produced some families of profiles for specific stall-regulated, variable pitch and variable-rpm wind turbines. Some of the NREL profiles information is available on their website (`https://wind.nrel.gov/airfoils/`). Other families of airfoils designed for HAWT are the Risø airfoils family (Fugslang and Bak, 2004) and the Delft airfoils family (Timmer and van Rooij, 2003).

1.3 Shear Center and Shear Stresses on Thin-Walled Beams

As presented on subsection 1.1, a necessary property to evaluate the constitutive matrix $\boldsymbol{D}$ is the shear center of the beam cross-section. The shear center is a specific point in the cross section where shear forces may be applied, producing no twist. Although this simple definition, the distribution of the shear stresses may be very complex regarding the material of the cross section, thickness considerations and the number of cells. More definitions about the shear center are found in works such as Pilkey (2002) and Fung (1993). The shear center referred to an arbitrary origin $\boldsymbol{O}$ may be defined, assuming the known shear stresses distribution $\boldsymbol{q} = \hat{\boldsymbol{q}}(A)$ from an applied shear force magnitude V, with components V_1 and V_2, in the cross-section plane. It is also possible to calculate each coordinate of the shear center separately. To calculate

the s_1 it is necessary to apply a shear force parallel to the axis 2 such as V_2. An analogue process also applies for the other beam section axis. Therefore, the shear center coordinates are:

$$s_1 = \frac{1}{V_2} \int_A |\boldsymbol{r} \times \boldsymbol{q}| dA \tag{7}$$

$$s_2 = \frac{1}{V_1} \int_A |\boldsymbol{r} \times \boldsymbol{q}| dA, \tag{8}$$

where $\boldsymbol{r}$ measures the distance between the origin $\boldsymbol{O}$ to the s element. Figure 4 presents a beam section, an arbitrary origin $\boldsymbol{O}$ and a thin-walled element s of the beam.

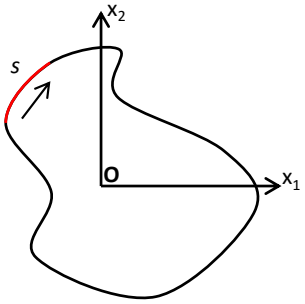

Figure 4: Beam thin-walled section and element s.

Thus, the major difficult arises from finding the shear stress distribution on the cross section of the beam. On this work, in order to reduce the complexity on finding the shear stress distribution, the thin-walled hypothesis is adopted. Furthermore, on this work the shear center follows the definition presented on Megson (2014) and expands it to a multicellular profile. The hypothesis adopted is that since the force is applied at the shear center each cell should have zero twist.

The thin-walled approach allows the consideration of constant stresses across the thickness of the beam. Other simplifications of this hypothesis is that squares and higher order terms of t are neglected on the section properties calculations and that the section is represented by its mid-line. Regarding the thin-walled assumption, according to Megson (2005) there is no exactly definition for a thin-walled structure, however it is pointed that the approximations are reasonably accurate for section which the ratio

$$\frac{t_{max}}{b} < 0.1 \tag{9}$$

where t_{max} is the maximum thickness of the section and b is a typical cross section dimension.

1.4 Torsion on Thin-Walled Beams

The last missing parameter for the constitutive matrix $\boldsymbol{D}$ presented on Subsection 1.1 is the torsion stiffness I_t. The torsion stiffness may be interpreted as the axial rotation stiffness of a given beam cross-section to an applied pure torque. It is defined as

$$GI_t = \frac{T}{\theta} \tag{10}$$

where T is the applied torque, G is the Shear Modulus and θ is the rate of twist of the section. Moreover, in order to calculate the torsion stiffness it is necessary to evaluate the rate of twist response to an applied torque. It is possible to prove, by equilibrium conditions, that a closed section thin-walled beam subject to a pure torque T, without axial constraints, has solution only for a constant shear flow q. On the case of a constant shear flow the rate of twist per unit length may be expressed as

$$\theta = \frac{q}{2GA} \oint \frac{ds}{t}, \tag{11}$$

where A is the enclosed area of the cell, ds is the differential thin-walled element and t is the thickness of the s element. Therefore, the torsion stiffness calculation of a single thin-walled profile may be summarized as:

1. Define a convenient rate of twist θ.
2. Calculate the equivalent shear flow q.
3. Calculate the torsion equivalent T.
4. Use equation 10 to calculate the torsion stiffness GI_t.

Although this simple process for the calculation of a single cell torsion stiffness, the multi-cellular torsion stiffness calculations are quite more complex. This work follows the the multi-cellular torsion stiffness definition presented by Shama (2010). The main hypothesis presented on this work is that each cell has the same twist per unit length. This condition generates one additional equation for each cell and makes the problem determined.

2 WIND TURBINE FEM MODEL

2.1 GIRAFFE

The GIRRAFE platform represents an advance on a previous finite element code named "FemCable", which main motivation was a finite element simulation of offshore structures, more specifically, the simulation of oil explotation risers. More information about the FemCable and their use is available at Gay Neto (2012).

The Generic Interface Readily Accessible for Finite Elements (GIRAFFE) is a generic platform for finite element analysis specially suitable for structural problems which may include translational and rotational DOFs and possible multiphysics applications (Gay Neto, 2015). Although GIRAFFE is not a fully generic platform, it was developed using the C++ object oriented language in a such way that new formulations, including translational and rotational DOFs, may be easily incorporated.

Furthermore, one of the finite element formulations available in GIRAFFE is the geometrically-exact beam presented on the subsection 1.1 which makes it a properly tool for the analysis of a highly nonlinear problem such as an HAWT dynamic simulation.

2.2 Wind Turbine Program

Although the simplicity of an beam-like model, some difficulties may arise to the assembly of an HAWT blade model. Some of the possible difficulties are:

- Varying airfoil shape along the blade.
- Calculation of geometric properties such as torsion stiffness and shear center of each cross-section.

The varying airfoil shape nature of an HAWT blade maybe an important issue since it has a huge variation along the length due to all structural requirements. Furthermore, the common use of webs on the cross section of HAWT blades may turn the calculation of the geometric properties such as the torsion stiffness and the shear center into a very laborious task.

In order to help on these issues it was developed a C# program with a GUI that helps on the geometric description of the blades for an HAWT. The program uses the thin-walled approximation and defines the profile by a set of points and the webs by the index of these points. The program interface is presented on Figure 5.

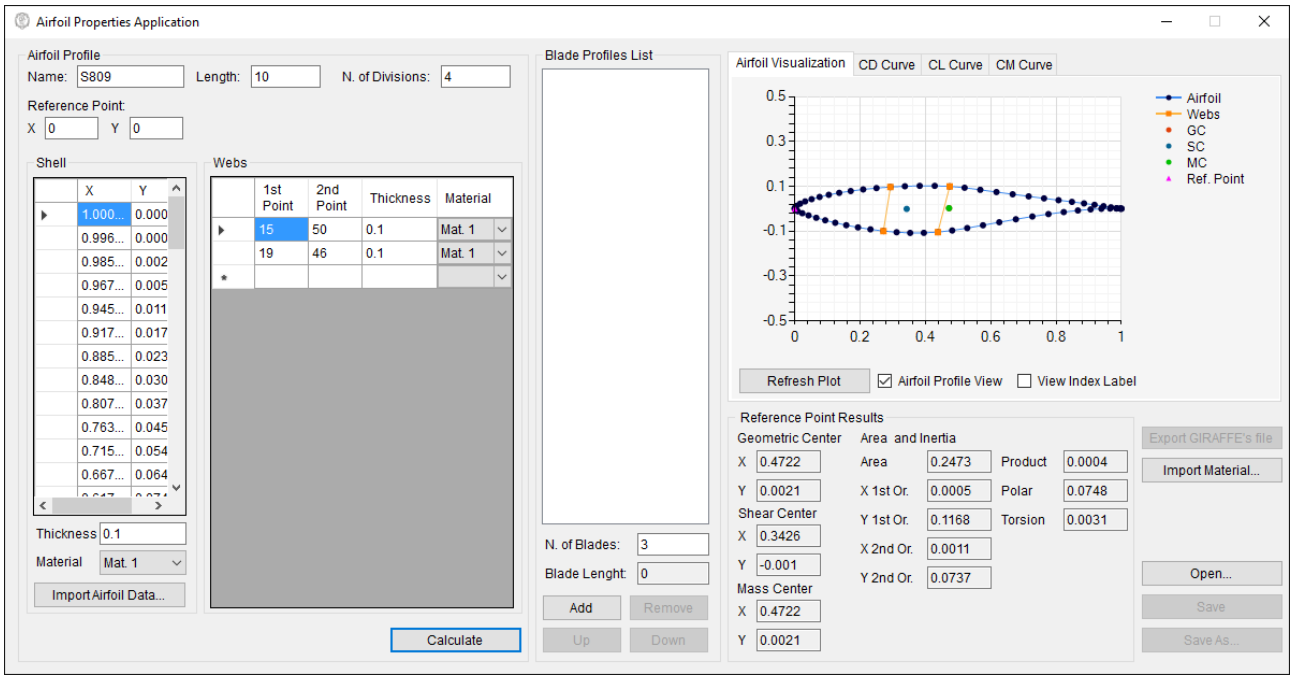

Figure 5: Wind Turbine GUI.

Some of the main features of the program are:

- Instant calculation of airfoil profile geometric properties.
- Permits the creation of a group of airfoil profiles.
- Permits the definition of any point as the beam axis.
- Exports all the necessary information to build the constitutive matrix for the GIRAFFE geometrically-exact beam formulation.

2.3 FEM Model Description

The aim of this subsection is to describe, in detail, all the characteristics that defines the wind turbine finite element model in analysis. This work presents dynamic simulation of the blades of an HAWT based on gravitational loads and a prescribed rotation on the central node of the wind turbine.

Some characteristics of the finite element model are:

- 3 equally-spaced wind turbine blades;
- 9 m length blade;
- 30 equally-spaced nodes per blade, total of 91 nodes;
- 3-node beam elements, total of 45 beam elements;
- 100 s simulation with integration time step of 0.01 s;
- 9.81 m/s^2 gravity acceleration to the negative z direction;
- Newmark integration method as presented on Ibrahimbegovic and Mikdad (1998) and Ibrahimbegovic and Mamouri (2000) with $\beta = 0.28$ and $\gamma = 0.54$.

In order to have a more realistic model, the local axis of each blade section is rotated on its containing plane. Table 1 summarizes the local vectors $\boldsymbol{e_1}$ and $\boldsymbol{e_3}$ that defines the local orientation of the cross-sections.

Blade	$\boldsymbol{e_1}$	$\boldsymbol{e_3}$
1	$(0, 0.9701, 0.2425)$	$(1, 0, 0)$
2	$(-0.2100, 0.9701, -0.1212)$	$(-0.5, 0, 0.8660)$
3	$(0.2100, 0.9701, -0.1212)$	$(-0.5, 0, -0.8660)$

Table 1: Local axis orientation of the blades.

The material properties of the blades has the following characteristics

- Young Modulus $E = 200$ GPa;
- Poisson coefficient $\nu = 0.3$;
- Density $\rho = 7500$ kg/m^3;

Although there is a known airfoil profile variation along the length of an HAWT blade, this work describes the blade using 4 profiles. The selection of these profiles is based on the NREL typical blades profiles described on Burton et al. (2011) for an stall regulated HAWT with diameter from 10 to 20 m. All the airfoil information used is available at the NREL website (`http://wind.nrel.gov/airfoils/`). The adopted thickness of the outer shell and the webs is 0.05 m. Table 2 summarize the profiles used on each beam section from 1 to 15 of the blade starting from the central node to the tip of the blade.

Beam	Airfoil Profile
1-2	16 point discrete circle (0.5 diameter)
3-7	NREL S807
8-12	NREL S805A
13-15	NREL S806A

Table 2: HAWT blade profiles.

Figure 6 presents the profiles used along the blade's length, their webs in red and the beam axis in green. The horizontal axis of of the profiles on Figure 6 represent the beam axis 1 and the vertical axis represent the beam axis 2 (see notation in Figure 1).

In order to evaluate the dynamics of the wind turbine structure some elements of the model will be monitored. In other words, these elements will have their displacements and reactions monitored on every time step of the simulation. On this work the monitored elements will be:

- Central wind turbine node (node 1);
- Tip node of each blade (nodes 31, 61 and 91);
- Beam element number 12;

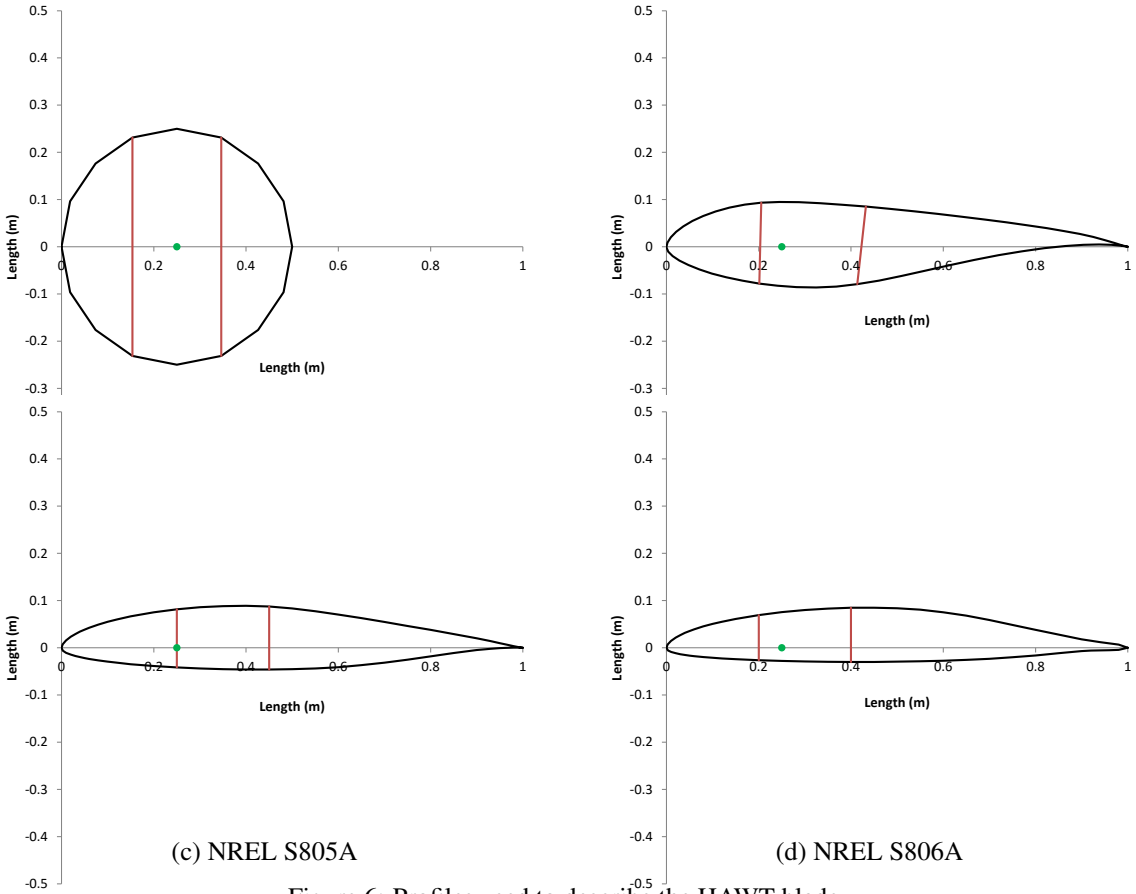

(c) NREL S805A (d) NREL S806A

Figure 6: Profiles used to describe the HAWT blade.

Figure 7 presents the wind turbine model and the monitors highlighted in red. The horizontal axis represents the x global orientation while the vertical axis represents the z global orientation and node 1 is at $(0, 0, 0)$.

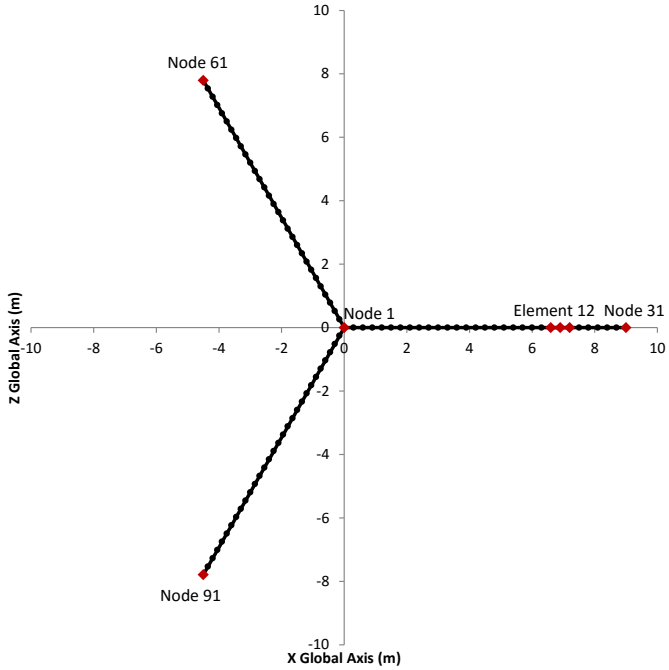

Figure 7: Wind turbine finite element model with monitors in red.

3 RESULTS

As previously described this dynamic simulation is induced by a prescribed rotation on the central node of the wind turbine. Although this simplification, the node 1 prescribed rotation expressed in radians is divided in 4 steps, described as follows:

- Step 1 - The rotation velocity increases from $t = 0s$ to $t = 20s$ according to the function $\phi_1(t) = 15\sin(0.025\pi t - \pi/2) + 15$;
- Step 2 - The rotation is velocity is maintained constant from $t = 20s$ to $t = 60s$, $\phi_2 = 15 + 1.2(t - 20)$;
- Step 3 - The rotation decreases from $t = 60s$ to $t = 80s$ according to the function $\phi_3(t) = 15\sin(0.025\pi t - \pi/2) + 63$;
- Step 4 - The rotation ceases from $t = 80s$ to $t = 100s$, $\phi_4 = 78$

Figure 8 presents a graphic that describes the node 1 rotation versus time. It is possible to note on this graph all the steps described previously.

On wind turbines the rotation of the blades yields on very important dynamic loads for the tower. These loads have huge influence on the structural behavior of an HAWT since they are crucial to evaluate aspects such as peak loads and fatigue. On this simulation the interface between the tower and the blades is monitored on node 1. Although the gravitational and inertial loads acting on the xz plane that contains the wind turbine blades, the axial peak forces occurred on the y direction. Figure 9 presents the y forces along time for node 1.

These peak loads may come from the way that the geometry of the blades was described. It follows that the centroid of each blade may not lie on the xz plane and that the axis of each blade is twisted on the plane of its cross section.

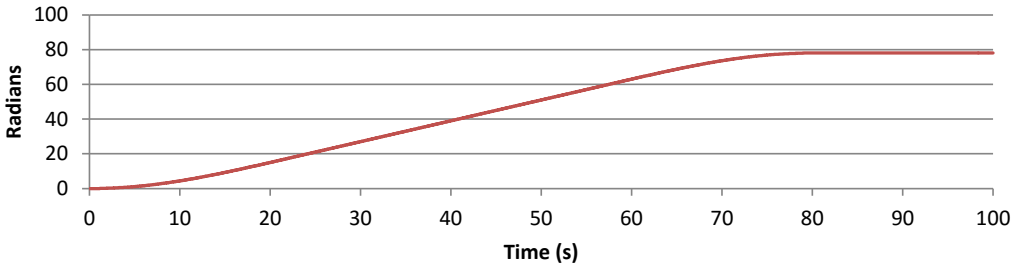

Figure 8: Node 1 rotation versus time.

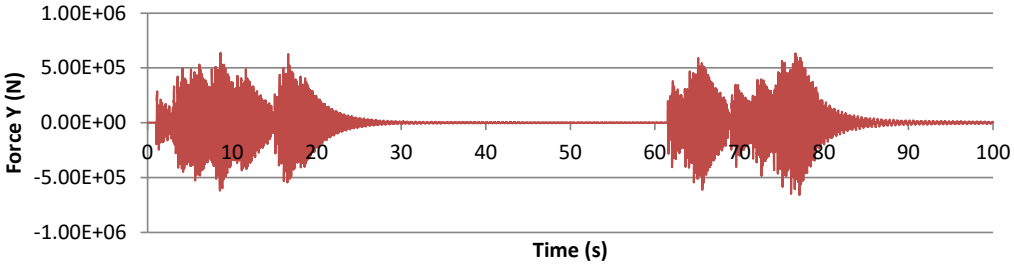

Figure 9: Force y along time.

It is also important to note that the peak loads occurs on step 1 and 3 that are the ones where there is change on the rotation velocity. This result is very interesting since the energy of a wind turbine comes from the motion resistance of the turbine inside the nacelle. Moreover, large force peaks may come from a severe acceleration/breaking operation applied to the rotor.

Figure 10 presents the z forces along time. It is seen on this graphic that the loads on the z direction are very relevant and include a non-null average, due to the structure self-weight. On steps 3 and 4 when the turbine is at a constant rotation speed and the turbine is stopped, the z direction force is the main force acting on node 1.

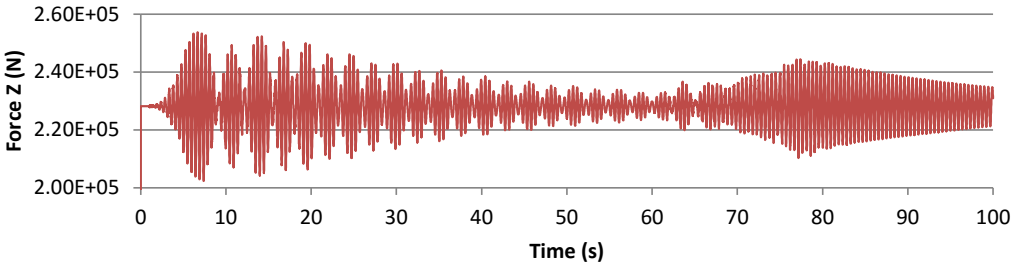

Figure 10: Force z along time.

Figure 11 presents the node 1 x forces along time. This graphic shows that although there are peak loads on steps 1 and 3, the highest peak loads are on step 4. The peak loads experienced

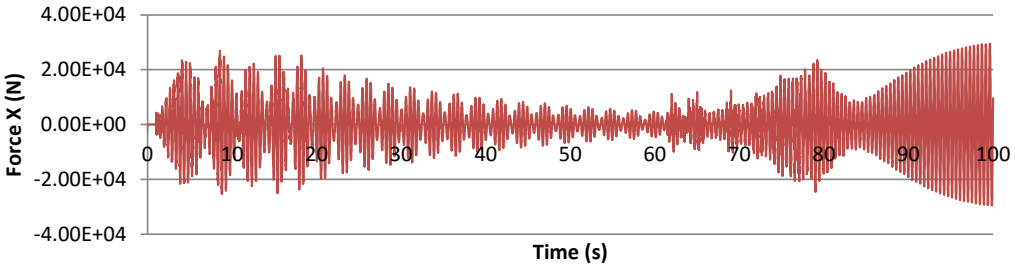

Figure 11: Force x along time.

on step 4 occurs due to the excitation of the blade tip and is considerably relevant.

One way to confirm the cyclic behavior of the dynamic model is by the analysis of the nodal displacement of each blade's tip. Figure 12 presents the x direction displacement of the nodes 31, 61 and 91.

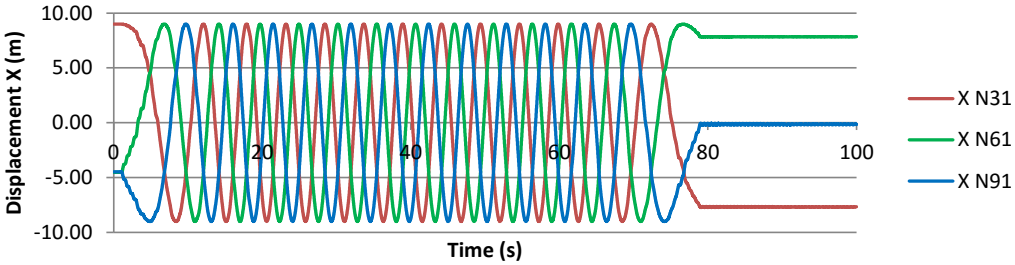

Figure 12: Displacement x along time of nodes 31, 61 and 91.

It is possible to note from this graphic that the turbine behaves as expected regarding the cyclic position of the coordinates. It is also interesting to note the node displacements when the turbine stops. Figure 13 presents a graphic of the x displacement of node 91 from $t = 80s$ to $t = 100s$. On this graphic is seen that the node position still oscillating, however tending to stop. This behavior was expected since there is an inherent numerical dumping on the simulation process due to the choice of Newmark integration parameters.

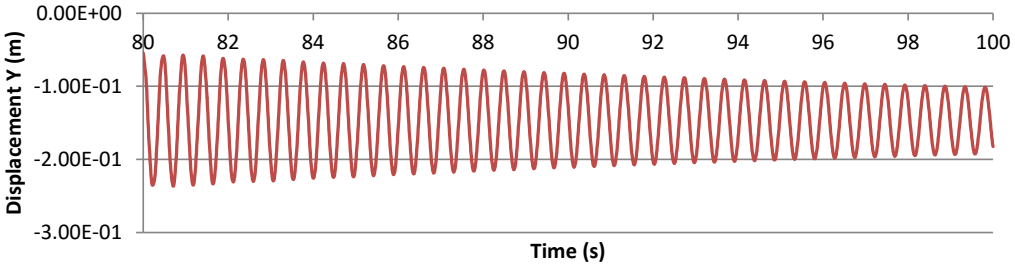

Figure 13: X displacement of node 91 from $t = 80$ to $t = 100$.

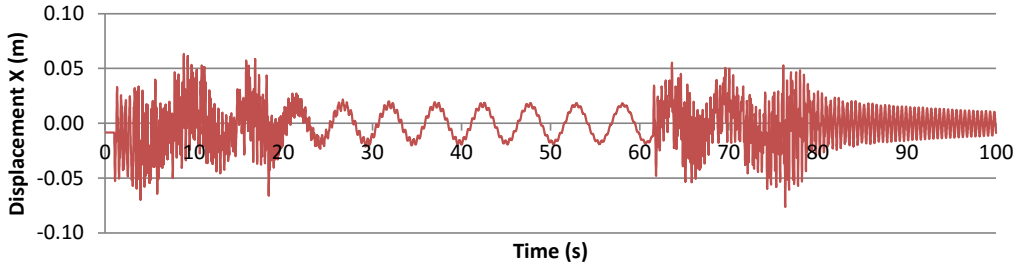

Figure 14: Y displacement of node 91 .

It is also interesting to see that the tip of the blade has out of plane displacements that appears from the geometry issues already discussed. Figure 14 presents the graphic that shows the out of plane displacement y of node 91. It seen that even when the wind turbine is at constant speed (step 2), there is an out of plane oscillating behavior of the node.

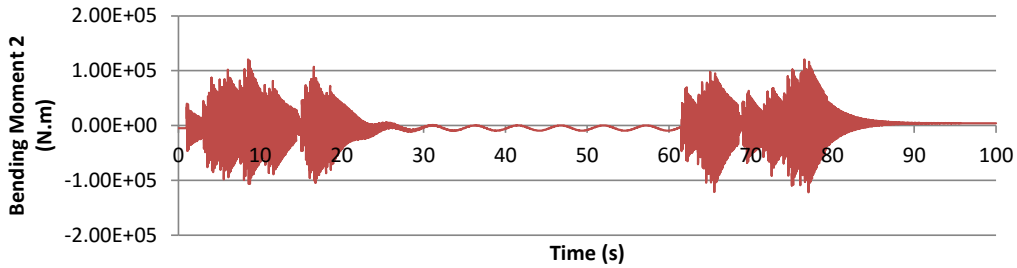

Figure 15: Bending moment around element axis 2 along time.

Despite of all the possible analysis of an HAWT dynamic simulation, the main usual goal is to evaluate the generalized stresses (tension, bending moment and torsion moment) acting on a specific part of the blade. On this simulation the part of interest on the blade structure is represented by the beam element 12. The bending moments around element axis 2 along time is shown on Figure 15. On this graphic is possible to note that the peak loads occurs when there is change on the rotation velocity of the wind turbine. It is also interesting to note that this bending moment still oscillating even when the rotation speed is constant (step 2).

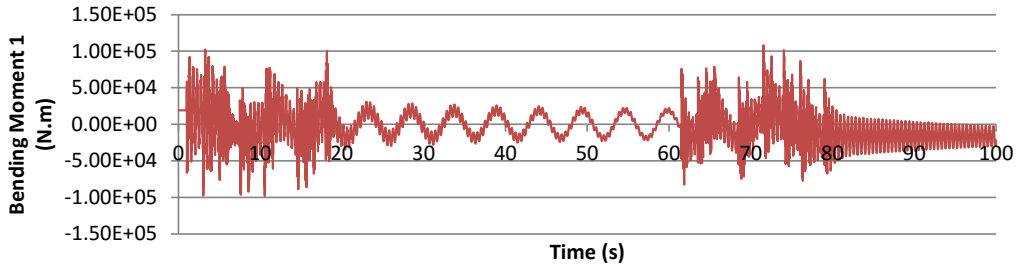

Figure 16: Bending moment around element axis 1 along time.

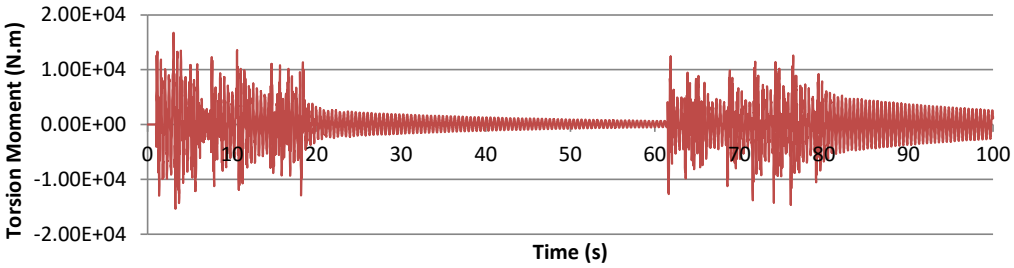

Figure 17: Torsion moment along time.

The bending moment around element axis 1 along time is presented on Figure 16. As other results, the peak loads are on steps 1 and 3. However the oscillating moment on step 4 indicates that the beam is still in movement.

Finally, the torsion moments along time is presented on Figure 17. Despite of the peak loads on steps 1 and 3, the torsion moments on step 4 are very relevant. Therefore, it is possible to assume that the stopping process of an wind turbine should be soft enough to avoid the possible high torsion moments on the blade.

4 CONCLUSION

The main conclusion of this work is that the GIRAFFE platform and the Wind Turbine program are very promising tools to evaluate the dynamics of an HAWT. The GIRAFFE geometrically-exact beam regarding the possibility of any cross section and beam axis position turns it into a very suitable tool for this kind of simulation. Furthermore, the user-friendliness of the Wind Turbine Program on handling defined cross sections and geometric properties calculations on a GUI is a very helpful tool for HAWT simulations.

Although on this simulation the aerodynamic loads were not included, it was seen that the variation of speed of an HAWT induces very relevant internal loads on the structure.

4.1 Future Works

Some of the possible advances regarding this work are:

- Verification of the thin-walled hypothesis;
- Verification of the shear center precision using shell elements;
- Verification of the torsion stiffness precision using shell elements;
- Inclusion of the aerodynamic loads.

4.2 Acknowledgments

The authors acknowledge FAPESP for funding this project under the grant number 2015/11655-3.

References

Burton, T., Jenkins, N., Sharpe, D., and Bossanyi, E. (2011). *Wind Energy Handbook*. John Wiley & Sons, Inc.

Fugslang, P. and Bak, C. (2004). Development of the risø wind turbine airfoils. *Wind Energy*, 7:142–162.

Fung, Y. C. (1993). *An Introduction to the Theory of Aeroelasticity*. Dover Publications Inc.

Gay Neto, A. (2012). Estabilidade estrutural da configuração estática de risers em catenária. Master's thesis, University of São Paulo.

Gay Neto, A. (2015). *Giraffe User's Manual*. University of São Paulo, v 1.0.100 edition.

Gay Neto, A. and Martins, C. A. (2013). Structural stability of flexible lines in catenary configuration under torsion. *Marine Structures*, 34:16–40.

Gay Neto, A., Pimenta, P. M., and Wriggers, P. (2014a). Contact between rolling beams and flat surfaces. *International Journal for Numerical Methods in Engineering*, 97(9):683–706.

Gay Neto, A., Pimenta, P. M., and Wriggers, P. (2014b). Self-contact modeling on beams experiencing loop formation. *Computational Mechanics*, 55:193–208.

Gere, J. M. and Timoshenko, S. (1997). *Mechanics of Materials*. PWS Publishing Company.

Hau, E. (2013). *Wind Turbines*. Springer.

Ibrahimbegovic, A. and Mamouri, S. (2000). On rigid components and joint constraints in nonlinear dynamics of flexible multibody systems employing 3d geometrically exact beam model. *Computer Methods in Applied Mechanics and Engineering*, 188(805-831).

Ibrahimbegovic, A. and Mikdad, M. A. (1998). Finite rotations in dynamics of beams and implicit timestepping schemes. *International Journal for Numerical Methods in Engineering*, 41(781-814).

Megson, T. H. G. (2005). *Structural and Stress Analysis*. ELSEVIER.

Megson, T. H. G. (2014). *Introduction to Aircraft Structural Analysis*. ELSEVIER.

Pilkey, W. D. (2002). *Analysis and Design of Elastic Beams*. John Wiley & Sons, Inc.

Pimenta, P. M. and Campello, E. (2001). Geometrically nonlinear analysis of thin-walled space frames. In *2nd European Congress on Computational Mechanics*.

Pimenta, P. M. and Yojo, T. (1993). Geometrically-exact analysis of spatial frames. *App. Mechanics Reviews*, 46(11):118–128.

Shama, M. (2010). *Torsion and Shear Stresses in Ships*. Springer.

Simo, J. C. (1985). A finite strain beam formulation. three-dimensional dynamic problem. part i. *Comp. Methods in App. Mech. and Eng.*, 49:55–70.

Simo, J. C. and Vu Quoc, L. (1991). A geometrically exact rod model incorporating shear and torsion-warping deformation. *Comp. Methods in App. Mech. and Eng*, 27(3):371–393.

Tangler, J. L. and Somers, D. M. (1995). *NREL Airfoil Families for HAWTs*. AWEA, Washington , DC.

Timmer, W. A. and van Rooij, R. P. J. O. M. (2003). ummary of the delft university wind turbine dedicated airfoils. *Journal of Solar Energy Engineering*, 125:488–496.

Timoshenko, S. and Goodier, J. N. (1951). *Theory of Elasticity*. McGraw-Hill.

Vlasov, V. Z. (1961). *Thin-Walled Elastic Beams*. Israel Program for Scientific Translations.

Wriggers, P., Gay Neto, A., and Pimenta, P. M. (2015). Modellierung von kabelstrukturen und deren verhalten bei kontakt und torsion. *Bauingenieur-Germany*, 90(193-199).

Yojo, T. (1993). *Análise Não-Linear Geometricamente Exata de Pórticos Espaciais*. PhD thesis, Polytechnic School at University of São Paulo.